Structure of Si atomic chains grown on the Si/Cu(110) $c(2\times2)$ surface alloy

C. Polop, C. Rojas, and J. A. Martín-Gago*
Instituto Ciencia de Materiales de Madrid-CSIC, Cantoblanco 28049-Madrid, Spain

R. Fasel, J. Hayoz, D. Naumović, and P. Aebi
Institut de Physique, Université de Fribourg, CH-1700 Fribourg, Switzerland
(Received 2 June 2000; published 1 March 2001)

The surface atomic structure of Si atomic chains grown on the Si/Cu(110) surface alloy has been investigated by a combination of different experimental techniques. For Si coverages below 0.5 monolayers the low-energy electron diffraction (LEED) pattern shows a $c(2\times2)$ reconstruction, corresponding to the formation of a surface alloy. Upon further Si deposition, the LEED pattern evolves toward a (2×2)-like structure with streaks along the [001] direction. Scanning tunneling microscopy (STM) images show the presence of linear atomic Si chains on top of the surface alloy layer. We present an atomic model for the surface termination based on the STM images and on the main atomic directions of the (2×2)-like phase found by a simple analysis of the Si $2p$ full hemispherical x-ray photoelectron diffraction patterns. This model consists of linear atomic Si chains running along the $[\bar{1}10]$ surface direction formed on top of the surface alloy. The chains present small (2×2) domains, which are not in phase with respect to each other. After heating the (2×2)-like phase up to 250 °C, a quasi-(3×4) structure is developed. This structure consists of similar chains exhibiting a different periodicity. Furthermore, we have used synchrotron radiation photoemission (x-ray and ultraviolet photoemission spectroscopy) to gather information about the electronic structure of the atomic chains.

DOI: 10.1103/PhysRevB.63.115414 PACS number(s): 68.35.Bs, 68.37.Ef, 79.60.−i

I. INTRODUCTION

The interface formed by depositing Si on a Cu substrate is of great technological and fundamental importance. The nature of the Schottky barrier is a fundamental problem in solid state science with important applications in the microelectronics technology. This is the reason why, in the last years, many metal–semiconductor interfaces have been studied by means of surface-sensitive methods, such as x-ray photoemission spectroscopy (XPS), Auger electron spectroscopy, or ultraviolet photoemission spectroscopy (UPS).[1,2] However, despite its technological importance and the great number of works devoted to this topic, no agreement has been found in explaining the origin of the Schottky barrier and the aspects dominating their magnitude. The role of the thickness and the number of defects at the interface could play an important role in the height determination.[3,4] For this reason, it is important to learn more about the first stages of interface formation and particularly about defects at the interface. Furthermore, a wealth of information is already available on metal-on-semiconductor interfaces but just a few works deal with the reversed deposition sequence, as in the present paper.[3,4] Hence, we have investigated the growth and the interface development *previous* to the Schottky barrier formation of Si deposited on a Cu(110) surface. Moreover, the Si–Cu interface has recently acquired great importance in microelectronics. The transition from Al– to Cu–interconnects in semiconductor manufacturing is rapidly taking place. Two primary factors drive this transition, the lower resistivity and the increased electromigration resistance that Cu offers relative to Al.[5] Thus, understanding the structural properties, growth mechanisms, and different phases between Si and Cu is an important issue for the microprocessor technology.

On the other hand, another motivation for this work is the fundamental study of a system presenting a low-dimensional structure. Linear atomic chains are of great importance because they can be thought as one-dimensional systems. The formation of atomic lines on well-characterized surfaces gives valuable information about self-organization processes and electron confinement along the chains. Recently, atomic dimmer chains have been reported for group III and IV metals deposited on Si(100).[6,7]

Recently it has been shown that room temperature deposition of 0.5 monolayers (ML) of Si deposited on a clean Cu(110) surface leads to the formation of a $c(2\times2)$ superstructure.[8] The surface atomic structure of the overlayer has been resolved by means of full-hemispherical x-ray photoelectron diffraction (XPD)[8] and quantitative low-energy electron diffraction (LEED).[9] It consists of an alternative substitution of the outmost Cu atoms from the $[\bar{1}10]$ rows by the deposited Si atoms. The Si atoms are slightly inward relaxed with respect to the Cu atoms. This atomic arrangement can be regarded as a surface alloy and it is schematically represented in Fig. 1(a). In this figure, shaded circles represent the deposited Si atoms. The (1×1) and the $c(2\times2)$ surface unit cells are also drawn. Figure 1(b) represents the corresponding LEED pattern. In this paper we are interested in the structures that are formed upon further Si deposition on the $c(2\times2)$ surface alloy, i.e., for Si coverages ranging between 0.5 and 0.8 ML. *A priori* several possibilities can be regarded. The arriving Si atoms could either form an ordered structure by bonding to Si atoms from the surface alloy in order to form a structure close to a Si bulk crystal or form amorphous Si clusters.

We have observed that deposition of about 0.2 Si ML on top of the $c(2\times2)$ superstructure [i.e., 0.7 ML of total Si coverage on clean Cu(110)] leads to the formation of a

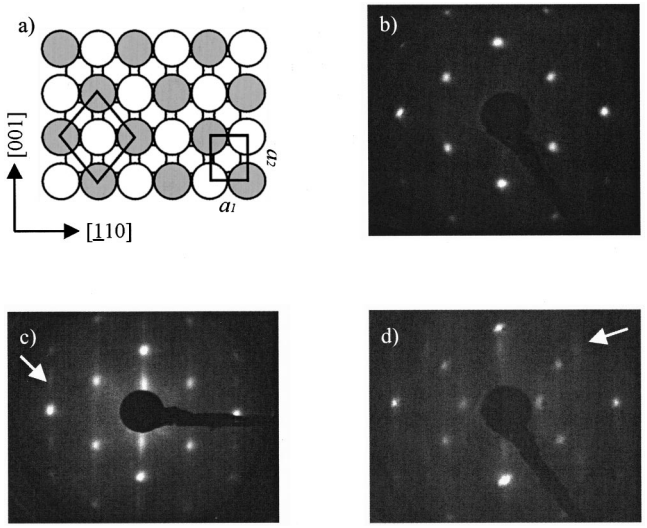

FIG. 1. (a) Schematic representation of the $c(2\times2)$ Si/Cu(110) surface alloy. Shaded circles represent the deposited Si atoms. The (1×1) and the $c(2\times2)$ surface unit cells are drawn. (b) The LEED pattern corresponding to the $c(2\times2)$ surface alloy. The beam energy is 70 eV. (c) The LEED pattern corresponding to the quasi-(2×2) structure. The beam energy is 70 eV. The arrow indicates the fractional spot (1,1/2). (d) The LEED pattern corresponding to the (3×4) structure. The beam energy is 60 eV. The arrow indicates the fractional spot (2/3,3/4).

streaked (2×2) LEED pattern overimposed on the $c(2\times2)$ pattern from the surface alloy. Streaks in the LEED pattern are associated with one-dimensional disorder, and thus, local probes should be employed for this type of study. As will be shown, the LEED streaks are related to a spot shape elongated along one of the high symmetry directions. Thus, from now on, we will call this structure quasi-(2×2). Further Si deposition leads to an unstructured LEED pattern indicating that the surface long-range order is lost. By combining several experimental techniques [LEED, scanning tunneling microscopy (STM), XPS, XPD] we will find out what is the surface atomic structure of the quasi-(2×2) phase and the atomic origin of the LEED pattern streaks. We will see that this structure consists of Si atomic chains running along the $[1\bar{1}0]$ surface direction, with the Si atoms placed on a center fcc site position. Furthermore, annealing of the quasi-(2×2) phase leads to the formation of a complicated (3×4) LEED pattern. STM and XPD experiments on this phase have revealed that similar chains, but with different periodicity, are also present in this case.

Hence, information about surface termination and local order has been gathered by STM, about the long-range order at the surface by LEED, and information about the adsorption site has been directly derived from full-hemispherical angle-scanned XPD. Furthermore, we have used synchrotron radiation photoemission (XPS and UPS) to characterize the electronic structure of the atomic chains.

The paper is organized as follows. First, a general description of the growth of Si on Cu(110) based on the LEED pattern evolution is given. Second, the two most important ordered phases are described on the basis of the STM images and XPD data, and an atomic model is proposed. Finally, a general discussion about the electronic properties of the chains formed in both phases is made.

II. EXPERIMENTAL DETAILS

Experiments were performed in three different experimental systems. One is equipped with STM and LEED $I-V$ techniques. The second with an ESCA-UPS analysis system where XPD patterns have been recorded. Finally, experiments were performed at the LURE (Laboratoire pour l'Utilisation du Rayonnement Electromagnétique) synchrotron radiation facility. All the STM images presented were recorded in topographic mode, and they have been slightly filtered (smoothed). Full-hemispherical XPD patterns were performed using a VG-ESCALAB Mk II spectrometer modified for motorized sequential angle-scanning data acquisition. Photoelectron spectra were recorded using Mg $K\alpha$ radiation ($h\nu=1253.6$ eV). Synchrotron radiation photoemission spectra were performed at the SA72 beamline in the Super-ACO (LURE) storage ring. The photon energy range was varied from 15 to 400 eV using different grating monochromators. Typical resolution (beamline plus analyzer) was around 200 meV at 100-eV photon energy.

The clean Cu(110) surface consists of rows of Cu atoms running along the $[1\bar{1}0]$ direction and presenting a (1×1) LEED pattern. This surface was prepared by the standard method of repeated cycles of Ar^+ sputtering and annealing at 600 °C Si was evaporated in the 10^{-10}-mbar range from a liquid nitrogen cooled electron bombardment evaporation cell which was calibrated before and after experiments with a quartz microbalance. Also, the Cu to Si x-ray photoelectron spectroscopy (XPS) intensity ratios matched the ones expected for the coverages.

III. EXPERIMENTAL RESULTS AND DISCUSSION

A. LEED pattern evolution with coverage

Figures 1(b)–1(d) show the LEED patterns of the different ordered structures at the Si–Cu(110) interface for submonolayer coverage. In all of them, the electron kinetic energy was set to 70 eV. Figure 1(b) shows the $c(2\times2)$ superstructure obtained after depositing approximately 0.5 ML Si at room temperature (RT). The real space $c(2\times2)$ unit cell responsible for the LEED pattern of Fig. 1(b) is sketched in Fig. 1(a).[8,9] As has already been indicated, this structure corresponds to an ordered surface alloy. This LEED pattern has low background intensity indicating that the surface alloy presents well-ordered and extended terraces.[10] Further Si deposition (around 0.8 ML of total Si coverage) on this overlayer leads to the formation of the streaked (2×2) LEED pattern represented in Fig. 1(c). The background has significantly increased with respect to the previous case. Streaks in a LEED pattern indicate that the surface structure is one-dimensionally disordered.[11] In this figure an arrow indicates the position of the (1,1/2) LEED spot. This spot is strongly elongated along the [001] direction, albeit a maximum of intensity is found for the 1/2 fractional position. For this reason this structure will be referred to as quasi-

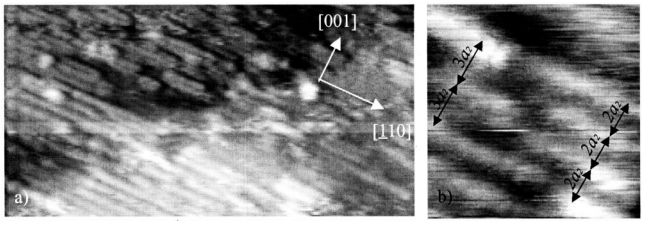

FIG. 2. Topographic STM images of the quasi-(2×2) structure formed for 0.8 Si ML deposited on Cu(110). Bias voltage 80 mV, tunnel current 0.9 nA. (a) General view of the surface. The total scanned area is 380×200 Å^2. (b) Region of the image showing the existence of chains on the surface. The scanned area is 45×42 Å^2.

(2×2). The LEED pattern of Fig. 1(d) was obtained after heating the quasi-(2×2) structure of Fig. 1(c) up to 250 °C. As in the previous case, the high background intensity and streaks indicate one-dimensional disorder. A quasi-(3×4) periodicity is observed in Fig. 1(d). The arrow on this figure indicates the position of a (2/3,3/4) fractional spot, which is narrower along the $[\bar{1}10]$ than along the [001] direction. Next, we will focus on describing the morphology of both ordered phases and on finding the atomic geometrical arrangements, which account for these LEED patterns.

B. The quasi-(2×2) phase

Figure 2(a) shows a general view of the surface presenting the quasi-(2×2) symmetry. The total scanned area is 380×200 Å^2. In this image we observe that the general morphology of the surface consists of close-packed atomic chains extending along the $[\bar{1}10]$ surface direction presenting many defects such as vacancies or unresolved clusters. All these imperfections are responsible for an increase of the LEED background intensity. Details of this surface is presented in Fig. 2(b). The total scanned area of this image is 45×42 Å^2 and some chains are seen closely. They are separated by different distances along the [001] direction. These distances are indicated in the figure, where ''a_2'' represents the modulus of the surface unit-cell vector of the substrate along the [001] direction ($a_2=3.61$ Å). The most frequently found distance is $2a_2$. As will be discussed next, this is the reason for the streaks along the [001] observed in the LEED pattern. The image also shows that the chains are not in phase with each other and they are about 100 Å long [see also Fig. 2(a)].

In order to understand more about the formation process and the atomic structure of the chains we have recorded STM images for coverages slightly higher than the surface alloy (i.e., at around 0.55 ML). Thus, it is easier to isolate an individual chain, avoiding confusion due to the coalescence of chains, which complicates the analysis of the structure. Figures 3(a)–3(c) show STM images recorded for a Si coverage of 0.55 ML. In these images information about the first stages of the formation of the quasi-(2×2) chains can be gathered. Figure 3(a) corresponds to a STM image recorded at 400 mV and with a scanned area of 330×280 Å^2. Two terraces, showing the $c(2\times2)$ structure separated by a

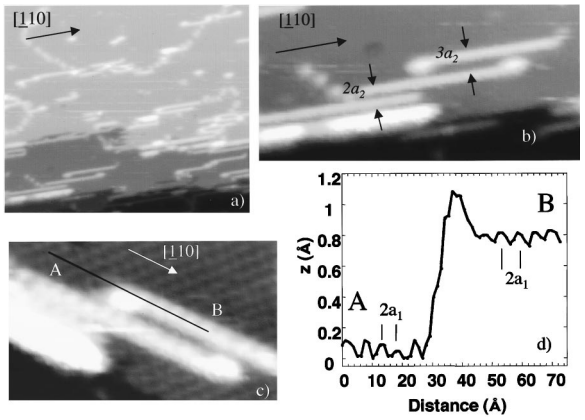

FIG. 3. Topographic STM images of the surface after deposition of 0.55 Si ML on Cu(110). Bias voltage 400 mV, tunnel current 1.5 nA. (a) A general view of the surface. The total scanned area is 330×280 Å^2. (b) The scanned area is 150×75 Å^2. (c) The scanned area is 100×50 Å^2. (d) Profile along the line represented in (c).

monoatomic step, are visible on the image. Additionally, some linear chains running along the $[\bar{1}10]$ direction are visible on the terraces. The average length of the chains is around 80 Å. The separation between consecutive chains is variable, ranging from 2 to 4 times the distance between $[\bar{1}10]$ Cu rows. Interestingly, it can be noticed that the chains start at a defect or unresolved cluster, which is imaged as a protrusion. All those facts suggest that the chains form by Si surface diffusion on the alloy terraces until the diffusing Si atom finds a defect (e.g., cluster, vacancy, or oxygen atom). This defect acts as a nucleation point that anchors the diffusing Si and makes the formation of Si chains possible. This could also be the reason for the absence of continuity of the chains visible in Fig. 2(b). We can confirm that the chains grow independently of each other and finally coalesce. Since the growth has started at different points, antiphase domains are formed. This can be seen in Fig. 3(b), where the separation between the three visible chains is different. Similar behavior (atomic chains starting at a defect) has been reported for the growth of Sn and Pb on Si(100).[6,12] For the case of Sn, this fact has been assigned to a different atomic adsorption site of the first atom of the chain.[6]

Figure 3(c) shows a detail of the image of Fig. 3(a) where the chain structure is appreciated. The scanned area is 100×50 Å^2. In this image an atomically resolved $c(2\times2)$ terrace is observed. The brilliant spots on the terraces correspond either to Si or Cu atoms because only one of the two different atoms that form the $c(2\times2)$ unit cell is imaged by the STM (see Fig. 1).[10] On top of the terrace two atomic chains showing a periodic structure are visible. The starting point of both chains appears as an extended feature, possibly indicating the starting defect from which the chain is formed. The distance between them is three times the distance between $[\bar{1}10]$ rows (i.e., $3a_2$). Figure 3(d) presents a profile along one of the chains indicated in Fig. 3(c) by a line. This figure shows that the periodicity between bumps in the chain and in the surface alloy terrace is the same, i.e., twice the modulus of the unit-cell vector a_1 ($a_1=2.55$ Å). The same distance between bumps along the chain is found in Fig.

2(b). The corrugation in the chain is around 0.1 Å, similar to the corrugation in the terrace. The height of the chain with respect to the terrace is around 0.7 Å. Although this value could be strongly affected by the different electronic structure of the chain with respect to the surface alloy, its magnitude is close to what is expected for a single atom deposited on the terrace. Thus, the STM images suggest that the chains consist of individual adatoms every two Cu bulk atoms along the $[1\bar{1}0]$ direction. Along this direction the periodicity is constant and it is at the origin of well-defined spots in the LEED pattern of Fig. 1(c) along this direction.

Summarizing the structural information obtained by the STM analysis, the quasi-(2×2) surface structure consists of atomic chains running along the $[1\bar{1}0]$ surface direction. The distance between atomic bumps is always twice the lattice parameter along the $[1\bar{1}0]$ direction but the separation between chains is variable, most of them are distant by two lattice distances along the [001] surface direction. However, the STM images do not give us any hint about the registry of the chains with the substrate.

Full hemispherical XPD is a powerful technique for obtaining structural information of surface overlayers. A visual inspection of XPD patterns recorded at high kinetic energies permits one to distinguish the directions where enhancement of emission is produced.[13] These peaks can be associated with forward scattering directions and, thus, they correspond to the main bonding directions of the sample under study. More details about the XPD technique and the measuring procedure can be found in Refs. 14 and 15. Figure 4(a) displays the experimental XPD pattern obtained by measuring the XPS Cu $3p$ emission intensity of a clean Cu(110) sample whereas Fig. 4(b) has been recorded for Si $2p$ for an approximate coverage of 0.8 ML Si and it corresponds to the LEED pattern of Fig. 1(c). The experimental kinetic energies for the Cu $3p$ and Si $2p$ emission lines are 1179 and 1153 eV, respectively. The patterns have been azimuthally averaged according to the twofold rotational symmetry of the system, and normalized with respect to the mean intensity for each polar emission angle. The angular distribution of the photoelectron intensity is plotted using the stereographic projection. The center of the plot corresponds to the surface normal and the outer circle represents grazing emission along the surface (90° off-normal emission). It is important to remark that the intensity has been measured up 88°. The $[1\bar{1}0]$ azimuth corresponds to the horizontal direction. In the XPD pattern from Fig. 4(a) the main Cu(110) crystallographic directions are found. This pattern has been deeply discussed in Ref. 14. In Fig. 4(b) intense forward scattering peaks are observed at polar emission angles of 60° with respect to the surface normal and at 55° off with respect to the azimuthal $[1\bar{1}0]$ direction (horizontal direction in the figure). They are labeled in Fig. 4 with capital letters. These four forward scattering peaks correspond to the low-index (011) crystallographic direction of the Cu crystal. Interestingly, for polar emission angles higher than 60° with respect to the surface normal, the XPD pattern shown in Fig. 4(b) presents the same features as the Cu $3p$ XPD pattern from Fig. 4(a) and corresponding to the clean surface. The XPD technique is giving information about the local environment around an emitter atom. As patterns for Si and Cu emitter atoms show the same features, one can affirm that the Si emitting atoms in the quasi-(2×2) structure have the same atomic environment as the Cu atoms in the clean Cu(110) surface. Furthermore, the absence of forward scattering emission for polar angles smaller than 60° indicates that the emitting Si atoms do not have a scatterer atom on top of them. Examining in detail the atomic structure of the Cu(110) surface and of the $c(2\times2)$ surface alloy, we can conclude that the emitter Si atom responsible for the diffraction pattern is the Si atom from the surface alloy which is underneath the atomic chains. This situation is illustrated in Figs. 4(c) and 4(d), where the main bonding directions responsible for the forward scattering peaks of Fig. 4(b) are indicated and labeled. Thus, the photoemission intensity of the Si $2p$ atoms from the surface alloy is forward focused by the adatoms in the chains. These facts clearly indicate that both emitter and scatterer Si atoms are placed at a center fcc position of the second and top layer, respectively, as shown in Figs. 4(c) and 4(d). This affirmation can be made without any calculation, because we deal with high-energy forward scattering peaks, in which the main contribution is geometrical.[13]

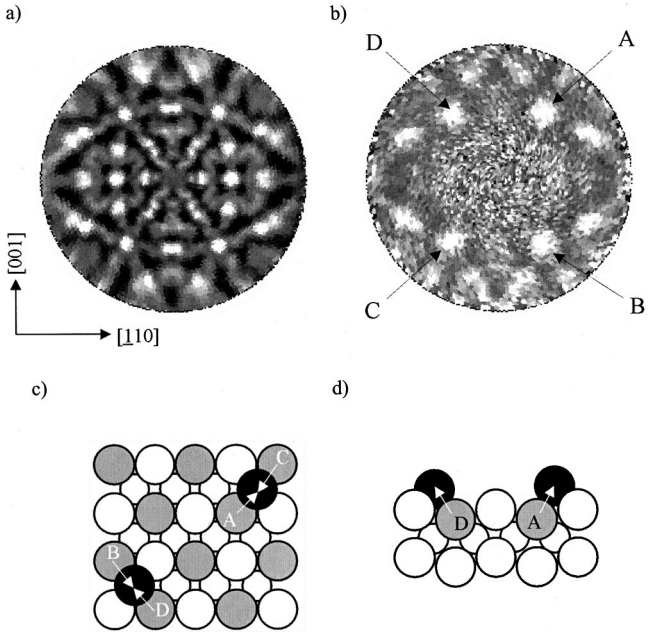

FIG. 4. Full angle XPD pattern of the (a) Cu $3d$ emission from a clean Cu(110) surface. Electron kinetic energy is 1179 eV. (b) Si $2p$ emission for a film 0.8 ML thick deposited on Cu(110) at room temperature. Electron kinetic energy is 1153 eV. Low index crystal directions and labels for the main forward scattering peaks are indicated. (c), (d) Schematic representation in top (c) and side view (d) of the bonding directions responsible for the peaks of (b).

The STM and XPD techniques together give information about the geometrical position of the scatters, not about the chemical nature of them. Thus, several possible models emerge from these experimental results. We cannot distinguish whether the scatter atom of the topmost layer is either a Cu or a Si atom or a mixture of both of them, i.e., whether the chains are made of Si, Cu, or both atoms are mixed in the chain. A Cu atom at the surface layer would indicate a sur-

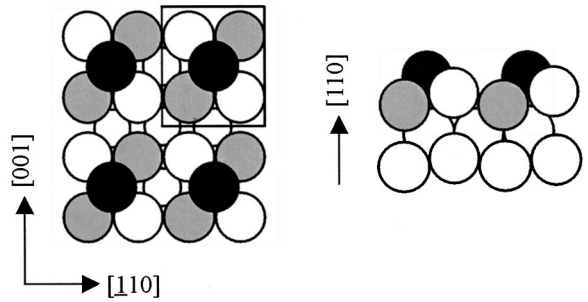

FIG. 5. Schematic representation of the proposed model for the (2×2) surface structure. Left part, top view. Right part, side view. Black filled circles represent Si atoms from the chains, shaded circles represent Si atoms from the surface alloy, and empty circles represent Cu atoms.

face segregation process. If this is the case, the surface layer will end in a double-layered surface alloy. However this model is unlikely because its formation will implicate RT diffusion toward the surface of the deep Cu atoms. The most probable model is to suppose that the extra Si atoms deposited occupy center fcc positions at the surface layer. To have information about the atoms in the chains we have studied the Si and Cu XPS intensity as a function of the coverage. We have seen that as Si is deposited the Cu XPS signal gets constantly attenuated, indicating that the deposited Si atoms remain on the surface.

Finally, and combining all the above-presented information by different techniques, we can propose an atomic model for the surface structure. We can conclude a quasi-(2×2) symmetry derived from the LEED pattern, the presence of chains and the interatomic distance obtained by STM images, a center fcc adsorption site derived from XPD, and a Si termination of this structure from XPS analysis. All these findings allow us to draw a unique geometrical model for the surface termination. This model is schematically represented in Fig. 5. Black filled circles represent Si atoms from the chains, shaded circles Si atoms from the surface alloy, and empty circles Cu atoms.

Once we have a model for the geometrical surface termination, we will focus on understanding the LEED streaks. As discussed previously, the LEED pattern is sampling the long-range order at the surface. The fact that the spots become streaked with Si coverage suggests one-dimensional disorder. However, this disorder is not reflected in the XPD pattern, which probes short-range order. The origin of the streaks becomes evident by analyzing the STM images. Figure 6 shows a sketch of the surface termination derived from the image of Fig. 2(b). The hairline represents the (2×2) unit cell. The dark balls represent the Si atoms from the chains. Although the most likely separation between chains is $2a_2$, other distances along the [100] surface direction such as $3a_2$ and $4a_2$ are found on the images (see Fig. 3). However, along the [110] row direction (along the Si chains), all atoms are separated by $2a_1$ Å. Thus, the separation between chains is not constant along the [100] direction suggesting that every chain is formed independently from each other and that an enhanced diffusion mechanism along the atomic rows at this temperature could be responsible for the higher

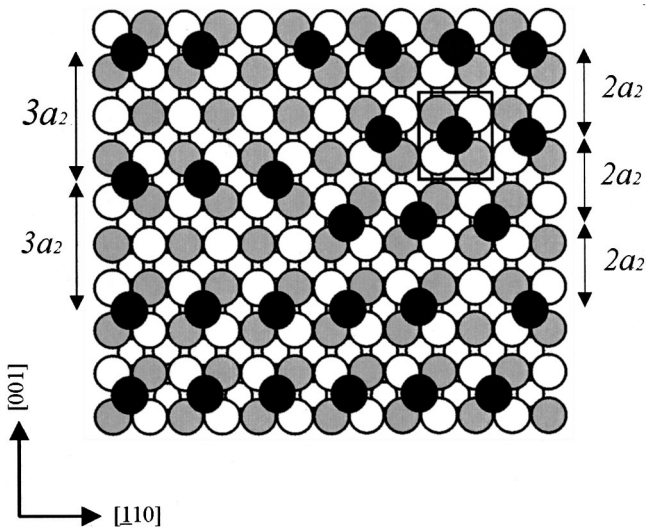

FIG. 6. Schematic representation of the image 2(b), indicating the origin of the one-dimensional disorder.

degree of order observed along the [110] direction. Other irregularities along [100] originate from different domains, as represented in the upper-right part of Fig. 6. In this case the chains are shifted by one position and then, they do not match each other anymore. All these irregularities cause the loss of long-range order along the [001] direction and as a consequence the appearance of streaks in the LEED pattern along this direction. Furthermore, the discussed features in the XPD pattern of Fig. 4(b) (labeled as A–D) show equal intensity instead of a symmetry breaking between A–C and B–D (Fig. 4) as could be derived from Fig. 5. That is, not only the A and C directions are detected as they should be, corresponding to a perfect, single-domain (2×2) structure but also B and D directions are appreciated. The existence of four symmetry directions, evidenced by the presence of four forward scattering peaks is additional proof of the existence of different domains.

The presence of different domains at the surface and one-dimensional disorder is responsible for the elongation of the LEED spots. The diameter, d, of the ordered structures contributing to the LEED pattern, i.e., the island size, is approximately determined through[11]

$$d = 0.88a\lambda/(w\sqrt{(a^2 - l^2\lambda^2)}),$$

where a is the periodicity along the studied direction (in our case $2a_2$), λ the electron wavelength, l the diffraction order, and w the full width at half maximum (FWHM) of the diffraction spot expressed in radians. Performing these calculations for the (1,1/2) spot of Fig. 1(c) we obtain a mean island width value of 26 Å for the quasi-(2×2) structure. This value corresponds to four scatters separated by a distance $2a_2$ along the [100] direction. The result can be compared in fair agreement (within error bars from piezo incertitude plus standard deviation) with the measured island size of 37 Å along the [100] direction in several STM images. This is an indication that the origin of the width of the spots is related to the island size.

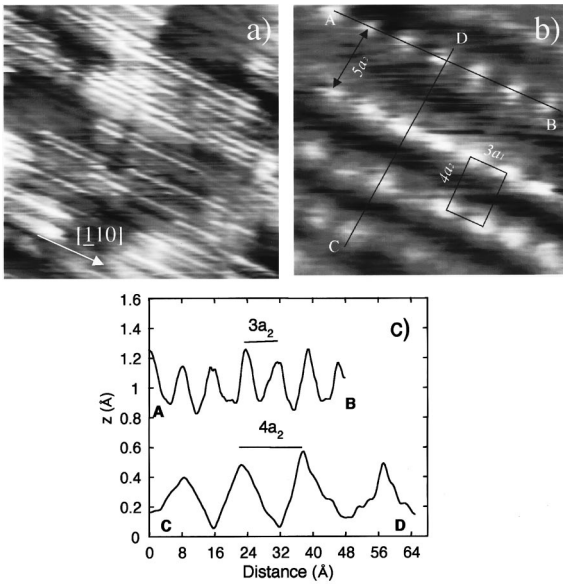

FIG. 7. Topographic STM images of the surface after deposition of 0.8 Si ML on Cu(110) and posterior annealing at 250 °C. Tunnel current 0.8 nA. (a) General view of the surface. The total scanned area is 480×480 Å^2. Bias voltage 480 mV. (b) Detail of the linear chains. The scanned area is 62×62 Å^2. Bias voltage 400 mV. (c) Profiles along the indicated directions of (b).

C. The quasi-(3×4) phase

Figure 1(d) shows the streaked 3×4 LEED pattern observed after depositing around 0.7 ML Si and then heating up the surface to temperatures around 250 °C. This structure will be referred to as the quasi-(3×4) phase.

The general topography of the surface, as observed by STM, consists of linear structures very similar to those found for the quasi-(2×2) surface. Figure 7(a) is a STM image showing a general view of the surface. The total scanned area in this image is 480×480 Å^2. The chains are longer along [1̄10] than for the quasi-(2×2) phase but more ordered along the [100] surface direction (perpendicular to the chains). Figure 7(b) shows details of those chains. The most frequent spacing between them is ''$4a_2$,'' although other longer distances are found. An analysis of several images shows that one can find different distances which are responsible for the streaks in the LEED pattern, as illustrated in Figs. 7(b) and 7(c). Figure 7(c) shows a profile along the two main surface directions as indicated in Fig. 7(b). The upper curve corresponds to a cut along the [1̄10] direction and the lower one along the [001] direction.

Moreover, the full hemispherical XPD pattern data recorded on this phase reflect the same symmetry as that found in Fig. 4 (data not shown), suggesting the presence of a similar chain structure. Thus, one can conclude that the atomic structure for both the 2×2 and the 3×4 phases is similar but the atomic periodicity within the chain is different. A tentative explanation for this longer periodicity could be related to the selective Si diffusion toward the Cu bulk. Indeed, we have reported in a previous work that annealing of the 2×2 phase (0.6 Si ML) to temperatures higher than 200 °C induces Si diffusion toward the bulk.[16] Additionally, the XPS ratio Si $2p$/Cu $3d$ is smaller than the ratio found for the quasi-(2×2) coverage, indicating that some Si atoms have disappeared during the annealing procedure.

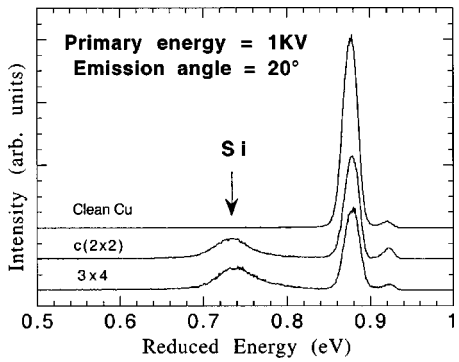

FIG. 8. Low-energy ion scattering spectroscopy spectra of the clean Cu(110) surface, $c(2\times2)$, and quasi-(3×4) structures as a function of the reduced energy (kinetic energy/primary energy).

In order to have an additional proof about the chain composition of the quasi-(3×4) phase we have performed ion scattering spectroscopy (ISS) at very low energy (1 keV). Due to the high neutralization probability of the ions, this technique is extremely surface sensitive.[17] In Fig. 8 ISS spectra are presented corresponding to the clean Cu surface (top), to the surface alloy (center, 0.5 Si ML), and to the quasi-(3×4) phase (bottom, 0.8 ML Si). Inclusion of Cu atoms in the chains will preserve the ratio of Si/Cu atoms at the surface, and then the ISS Cu to Si signal ratio will be the same with respect to the surface alloy. However, this is not observed in Fig. 8. The attenuation of the Cu peak for the quasi-(3×4) phase indicates that the chains formed on the surface are Si chains. The Cu signal is coming from the Si–Cu surface alloy, which is visible because of the very open fcc(110) structure (see Fig. 5). This observation is in agreement with the XPS ratio evaluation, and it is an additional proof for the Si composition of the (3×4)-like chains.

D. Some considerations about the electronic structure of the chains

The XPS technique gives information about the chemical species present in the surface region of a sample. Figure 9 represents the Si $2p$ core-level photoemission spectra for the different structures under study. The photon energy was set at 180 eV. The upper spectrum corresponds to the $c(2\times2)$ surface alloy. The two maxima are split by 0.6 eV and they correspond to the Si $2p1/2$ and Si $2p3/2$ components. These components are indicated in Fig. 9 by two parallel thick lines separated by 0.6 eV. On the left-hand side of the spectrum a shoulder indicates the presence of small components which are shifted. A previous high-resolution core-level photoemission study[10] has shown that the Si $2p$ peak can be decomposed in four different peaks, associated with different atomic environments (islands, clusters). The main peak has been taken as energy reference and it corresponds to the surface alloy. Due to the high degree of order of the surface alloy, the Si $2p$ core-level peak is very narrow (The narrowest FWHM reported in literature for a Si $2p$ core level peak

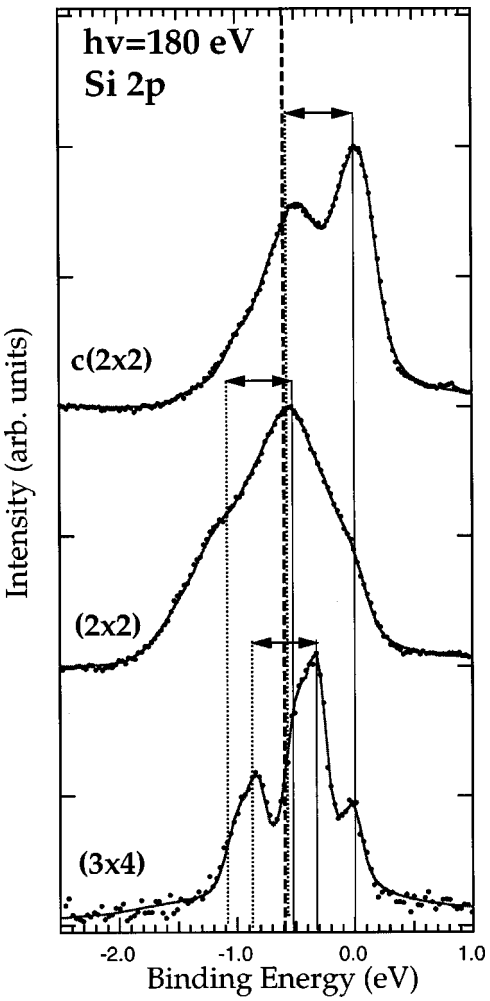

FIG. 9. Si $2p$ core level photoemission peak for the $c(2\times2)$ surface alloy, quasi-(2×2), and quasi-(3×4) structures. The best fit is represented by a thin solid line overlapping the experimental points. The dotted vertical line represents the position of a bulk Si crystal. The thick lines at the bottom of every spectrum represent the main components of the Si $2p1/2$ and Si $2p3/2$ split by 0.6 eV.

in the solid state is reported in Ref. 10 for this surface alloy). The binding energy of the Si $2p$ level measured from a Si(111) crystal (bulk peak) in our experimental configuration is 0.62 eV shifted with respect to the surface alloy peak toward the high binding energy side of the spectrum and its binding energy is marked in Fig. 9 by a dotted line. We believe that this difference is related to extra atomic relaxation effects rather than to a charge transfer process from Cu to Si. Core level shifts up to 5 eV induced by screening have been theoretically predicted for a Si adatom on a high-density metal surface (jelium).[18] Additionally, a 0.4-eV shift in the Si $2p$ peak from a metallic $ErSi_{1.7}$ exclusively induced by extra-atomic effects has been reported.[19] The surface alloy is similar in the sense that in both materials Si atoms are forming a metallic bidimensional system.

The central spectrum in Fig. 9 corresponds to the quasi-(2×2) phase. The maximum of this peak appears shifted with respect to the surface alloy by 0.54 eV, and its binding energy is very close to the Si bulk binding energy. The peak corresponding to the surface alloy is still present and it is visible as a shoulder, indicating that the quasi-(2×2) phase is not destroying the surface alloy but growing on top of it. This observation is in agreement with the model proposed in Fig. 5 where the surface alloy exists below the Si chains. Moreover, the XPS peak has broadened, indicating higher disorder with respect to the surface alloy phase. The shift of 0.54 eV toward higher binding energies indicates that the atomic environment of Si in the quasi-(2×2) phase is closer to that of Si bulk. Si atoms in the chains have two Si atoms from the surface alloy as neighbors (see Fig. 5). It is important to note the possibility at this energy to also find the signal from amorphous Si clusters associated with defects.

When the quasi-(3×4) phase is formed (lower spectrum in Fig. 9), the maximum of the XPS appears at 0.35 eV from the energy reference, i.e., 0.2 eV shifted toward lower binding energies with respect to the quasi-(2×2) phase. This indicates that the Si atoms of the chains feel stronger the metallicity of the surface alloy underneath. Furthermore, the $c(2\times2)$ structure is also visible and well resolved. Peaks are narrower indicating that this structure presents a higher degree of order than the quasi-(2×2) phase. Although the maximum appears at 0.35 eV from the surface alloy peak, a shoulder is seen at 0.54 eV indicating that some Si chains with a 2×2 periodicity are still present in the surface.

It is very difficult to obtain information about the electronic structure of individual chains. STM is a technique that could offer this information. However, it is not clear whether the tunneling current comes from the metallic surface alloy that supports the chain or from the Si chain itself. Thus, we did not interpret changes in the chain topography induced by the bias voltage, indicating the absence of localized dangling bonds or π-type states. However, we have measured synchrotron radiation ultraviolet photoemission spectra for different stages of the growth. In Fig. 10 we show the valence band evolution for different Si coverages recorded in normal emission for a photon energy of 21 eV. The bottom spectrum corresponds to the clean Cu surface and it is characterized by the strong emission of the $3d$ levels at around -2.3 eV of binding energy. The surface alloy phase is electronically characterized by the appearance in the valence band of two new states, labeled as Si1 and Si2 in Fig. 10. Both have been deeply discussed in a previous publication.[20] In that work, by means of local density of states calculations, the Si1 peaks were assigned to two-dimensional states characteristic of this surface structure. The state Si1 consists of two close peaks located at -0.9 and -1.2 eV of binding energy. These two peaks have higher intensity when the $c(2\times2)$ LEED spots are sharper, for an approximate coverage of 0.5 ML (surface alloy formation). The peak labeled as Si2 consists of a broad structure centered at around -3.0 eV. We also find a net increase in the total number of counts at the Fermi level with coverage, indicating that the formed alloy is metallic. Si1 states disappear when the quasi-(2×2) phase is formed, and the peak labeled as Si2 increases strongly. We know that this peak has an important contribution from Si $2p$ states.[20] A very tiny state, labeled as Si3, appears in the quasi-(2×2) phase at -1.5 eV. This peak may be characteristic of the Si chains. This state does not disperse with photon energy (data

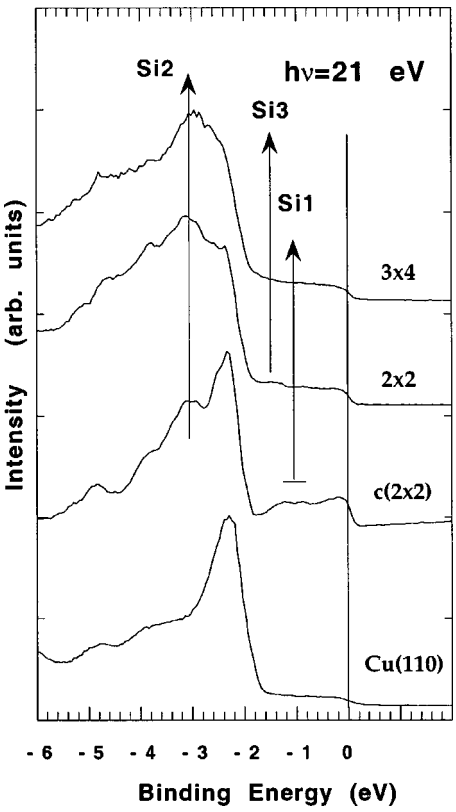

FIG. 10. Valence band photoemission spectra recorded at normal emission for the different structures indicated. Photon energy: 21 eV.

not shown), indicating its bidimensional character, and therefore, may be assigned to a surface state characteristic of the Si-chains. The Si3 state disappears at the quasi-(3×4) phase. It is clear from the figure that the number of counts at the Fermi edge drops when Si chains are formed. This is an indication of a predominant Si–Si semiconducting bonding between the Si in the chains and the metallic Si from the surface alloy.

Si chains have been reported as a metastable reconstruction of the cleaved Si(111) 2×1. The surface structure is characterized by quasi-one-dimensional zigzag chains of Si atoms bonded by π orbitals.[21,22] For this reason the chains have been called Si π chains. The Si π chains exhibit important electronic effects if the tunnel voltage is reversed, induced by bonding and antibonding states.[22] However, this is not the case for the Si chains presents at the Si–Cu interface. We did not find any change in the chain topography induced by the bias voltage. Moreover, for the Si π chains at the Si(111) 2×1 surface the corrugation within the chain varies from 0.05 to 0.6 Å, depending on the bias voltage and tip sharpness.[21] In the case under study, the corrugation within the chain for any tried voltage is around 0.1 Å (see Fig. 3). Both the absence of electronic effects and low corrugation, indicate the lack of localized states on the Si chains formed on the Si–Cu interface and suggest a high hybridization with the substrate.

IV. CONCLUSIONS

Si deposited on the ordered and well-characterized Si/Cu(110) surface alloy forms Si chains characterized by a streaked (2×2) LEED pattern. These chains run along the $[1\underline{1}0]$ surface direction and they form (2×2) domains without coherence between them. The combination of experimental results from different techniques allows us to present an atomic model for the geometrical structure of the chains. The surface alloy structure is preserved and the Si chains are grown on top of it in a center fcc position. Similar chains are found after heating the quasi-(2×2) phase up to 250 °C but exhibiting a (3×4) periodicity.

ACKNOWLEDGMENTS

Skillful technical assistance was provided by E. Mooser, O. Raetzo, H. Tschopp, Ch. Neururer, and F. Bourqui. This project has been supported by the Fonds National Suisse pour la Recherche Scientifique. One of us (J.A.M.-G.) is grateful to the Institut de Physique de l'Université de Fribourg for financial support. This research project was included within the frame of the Spanish CICYT Project No. PB98/0524. We are grateful to the SA72LURE staff for its assistance during the measurements.

*Author to whom correspondence should be addressed; Email: Gago@icmm.csic.es

[1] L. J. Brillson, Surf. Sci. Rep. **2**, 123 (1982).
[2] M. Heineman, Surf. Rev. Lett. **1**, 429 (1994).
[3] Y. Chang, Y. Hwu, J. Hansen, F. Zanini, and G. Margaritondo, Phys. Rev. Lett. **63**, 1845 (1989).
[4] R. Dudde, H. Bernhoff, and B. Reihl, Phys. Rev. B **41**, 12 029 (1990).
[5] X. W. Lin and Dipu Pramanik, Solid State Technol. **41**, 63 (1998).
[6] J. C. Glueckstein, M. M. R. Evans, and J. Nogami, Surf. Sci. **415**, 80 (1998).
[7] P. F. Lyman and M. J. Bedzyk, Surf. Sci. **371**, 307 (1997).
[8] J. A. Martín-Gago, R. Fasel, J. Hayoz, R. G. Agostino, D. Naumović, P. Aebi, and L. Schlapbach, Phys. Rev. B **55**, 12 896 (1997).
[9] C. Polop, C. Rojas, E. Román, J. A. Martín-Gago, B. Brena, D. Cocco, and G. Paolucci, Surf. Sci. **497**, 268 (1998).
[10] J. A. Martín-Gago, C. Rojas, C. Polop, J. L. Sacedón, E. Román, A. Goldoni, and G. Paolucci, Phys. Rev. B **59**, 3070 (1999).
[11] G. Ertl and K. Küppers, *Low Energy Electrons and Surface Chemistry* (VCH, Weinheim, 1985).
[12] J. Y. Veuillen (private communication).
[13] J. Osterwalder, P. Aebi, R. Fasel, D. Naumović, P. Schwaller, T. Kreutz, L. Schlapbach, T. Abukawa, and S. Kono, Surf. Sci. **331**, 1002 (1995).
[14] J. Hayoz, Th. Pillo, R. Fasel, L. Schlapbach, and P. Aebi, Phys. Rev. B **59**, 15 975 (1999).
[15] D. Naumović, A. Stuck, T. Greber, J. Osterwalder, and L. Schlapbach, Phys. Rev. B **47**, 7462 (1993).
[16] C. Rojas, F. J. Palomares, M. F. López, A. Goldoni, G. Paolucci, and J. A. Martín-Gago, Surf. Sci. **454–456**, 778 (2000).

[17] J. A. Martin-Gago, F. Comin, and S. Ferrer, Surf. Sci. **369**, 45 (1996).
[18] A. R. Willians and N. D. Lang, Surf. Sci. **68**, 138 (1977).
[19] J. A. Martín-Gago, J. M. Gomez-Rodriguez, and J. Y. Veuillen, Phys. Rev. B **55**, 5136 (1997).
[20] C. Rojas, J. Cerdá, I. Jimenez, M. Martín, and J. A. Martín-Gago, Surf. Sci. **466**, 199 (2000).
[21] J. A. Stroscio, R. M. Feenstra, and P. Fein, J. Vac. Sci. Technol. A **5**, 838 (1987).
[22] J. A. Stroscio, R. M. Feenstra, and P. Fein, Phys. Rev. Lett. **57**, 2579 (1987).